International Journal of Mathematical Archive-8(1), 2017, 15-25
Available online through www.ijma.info ISSN 2229 – 5046

EFFECT OF HEAT SOURCES ON NON-DARCY CONVECTIVE HEAT AND MASS TRANSFER FLOW IN A VERTICAL CHANNEL

C. SULOCHANA, G. N. RAMAKRISHNA*

Department of Mathematics, Gulbarga University, kalaburagi, Karnataka, India.

(Received On: 12-12-16; Revised & Accepted On: 13-01-17)

ABSTRACT

An attempt has been made to investigate the chemical reaction effects on Non-Darcy convective heat and Mass transfer flow of a viscous fluid in a vertical channel with heat generating sources. The governing equations of flow, heat and mass transfer have been solved by using Galerkin finite element analysis with Quadratic Polynomial approximations. The velocity, temperature, concentration, shear stress and rate of Heat and Mass transfer are evaluated numerically for different variations of parameter. It is found that the inclusion of inertia effects is to reduce the velocity and increase the temperature and concentration in the flow region. The velocity, temperature and concentration experience an enhancement with increase in the strength of the heat generating source and reduce with that of heat absorption.

Key Words: *Non-Darcy flow, Heat sources, Porous Medium, Chemical Reaction.*

1. INTRODUCTION

The study of heat generation or absorption effects in moving fluids is important in view of several physical problems such as fluid undergoing exothermic or endothermic chemical reactions. The volumetric heat generation has been assumed to be constant or a function of space variable. For example, a hypothetical core – disruptive accident in a liquid metal fast breeder reactor (LMFBR) could result in the setting of fragmented fuel debris on horizontal surfaces below the core. The porous debris could be saturated sodium coolant and heat generation will result from the radioactive decay of the fuel particulate.

Vajravelu and Hadjinicolaou [31] studied the heat transfer characteristics in the laminar boundary layer of a viscous fluid over a stretching sheet with viscous dissipation or frictional heating and internal heat generation. Hossain et al [17] studied the problem of natural convection flow along a vertical wavy surface with uniform surface temperature in the presence of heat generation or absorption. Alam *et al.* [1] studied the problem of free convection heat and mass transfer flow past an inclined semi-infinite heated surface of an electrically conducting and steady viscous incompressible fluid in the presence of a magnetic field and heat generation. Chamkha [8] investigated unsteady convective heat and mass transfer past a semi-infinite porous moving plate with heat absorption. Hady *et al.* [16] studied the problem of free convection flow along a vertical wavy surface embedded in electrically conducting fluid saturated porous media in the presence of internal heat generation or absorption effect.

The vertical channel is a frequently encountered configuration in thermal engineering equipment, for example, collectors of solar energy, cooling devices of electronic and micro-electronic equipments etc. The influence of electrically conducting the case of fully developed mixed convection between horizontal parallel plates with a linear axial temperature distribution was solved by Gill and Casal [13]. Ostrach [21] solved the problem of fully developed mixed convection between vertical plates with and without heat sources. Cebeci *et al.* [7] performed numerical calculations of developing laminar mixed convection between vertical parallel pates for both cases of buoyancy aiding and opposing conditions. Wirtz and McKinley [32] conducted an experimental study of an opposing mixed convection between vertical parallel plates with one plate heated and the other adiabatic. Al-Nimir and Haddad [2] have described the fully developed free convection in an open-ended vertical channel partially filled with porous material. Greif *et al.* [14] have made an analysis on the laminar convection of a radiating gas in a vertical channel. Gupta and Gupta [15] have studied the radiation effect on a hydromagnetic convective flow in a vertical channel. Datta and Jana [11] have studied the effect of wall conductance on a hydromagnetic convection of a radiation gas in a vertical channel. The combined forced and free convective flow in a vertical channel with viscous dissipation and isothermal –isoflux boundary conditions have been studied by Barletta [3]. Barletta *et al.* [4] have presented a dual mixed convection flow in a vertical channel. Barletta *et al.* [5] have described a buoyancy MHD flow in a vertical channel.

Corresponding Author: G. N. Ramakrishna*

Non – Darcy effects on natural convection in porous media have received a great deal of attention in recent years because of the experiments conducted with several combinations of solids and fluids covering wide ranges of governing parameters which indicate that the experimental data for systems other than glass water at low Rayleigh numbers, do not agree with theoretical predictions based on the Darcy flow model. This divergence in the heat transfer results has been reviewed in detail in Cheng [9] and Prasad *et al.* [23] among others. Extensive effects are thus being made to include the inertia and viscous diffusion terms in the flow equations and to examine their effects in order to develop a reasonable accurate mathematical model for convective transport in porous media. The work of Vafai and Tien [29] was one of the early attempts to account for the boundary and inertia effects in the momentum equation for a porous medium. They found that the momentum boundary layer thickness is of order of $\sqrt{\frac{k}{\varepsilon}}$. Vafai and Thiyagaraja [30] presented analytical solutions for the velocity and temperature fields for the interface region using the Brinkman Forchheimer –extended Darcy equation. Detailed accounts of the recent efforts on Non-Darcy convection have been recently reported in Tien and Hong [26], Cheng [9], Kalidas and Prasad [18]. Here, we will restrict our discussion to the vertical cavity only. Poulikakos and Bejan [24] investigated the inertia effects through the inclusion of Forchheimer velocity squared term, and presented the boundary layer analysis for tall cavities. They also obtained numerical results for a few cases in order to verify the accuracy of their boundary layer analysis for tall cavities. They also obtained numerical results for a few cases in order to verify the accuracy of their boundary layer solutions. Later, Prasad and Tuntomo [22] reported an extensive numerical work for a wide range of parameters, and demonstrated that effects of Prandatl number remain almost unaltered while the dependence on the modified Grashof number, Gr, changes significantly with an increase in the Forchheimer number. This result in reversal of flow regimes from boundary layer to asymptotic to conduction as the contribution of the inertia term increases in comparison with that of the boundary term. They also reported a criterion for the Darcy flow limit.

The Brinkman – Extended – Darcy modal was considered in Tong and Subramanian [27], and Lauriat and Prasad [20] to examine the boundary effects on free convection in a vertical cavity. While Tong and Subramanian performed a Weber – type boundary layer analysis, Lauriat and Prasad solved the problem numerically for A=1 and5. It was shown that for a fixed modified Rayleigh number, Ra, the Nusselt number; decrease with an increase in the Darcy number; the reduction being larger at higher values of Ra. A scale analysis as well as the computational data also showed that the transport term $(v.\nabla)v$, is of low order of magnitude compared to the diffusion plus buoyancy terms. A numerical study based on the Forchheimer-Brinkman-Extended Darcy equation of motion has also been reported recently by Beckerman *et al.* [6]. They demonstrated that the inclusion of both the inertia and boundary effects is important for convection in a rectangular packed – sphere cavity. Umadevi *et al.* [28] have studied the chemical reaction effect on Non-Darcy convective heat and mass transfer flow through a porous medium in a vertical channel with heat sources. Deepthi *et al.* [12] and Kamalakar *et al.* [19] have discussed the numerical study of non-Darcy convective heat and mass transfer flow in a vertical channel with constant heat sources under different conditions. Recently Sreenivasa Rao [] have discussed the effect of Non-Darcy convective heat and mass transfer flow in a vertical channel.

Keeping the above application in view we made an attempt to study chemical reaction effects on Non-Darcy convective heat and Mass transfer flow of a viscous fluid in a vertical channel with heat generating sources. The Brinkman Forchheimer extended Darcy equations which take into account the boundary and inertia effects are used in the governing linear momentum equation. In order to obtain a better insight into this complex problem, we make use of Galerkin finite element analysis with Quadratic Polynomial approximations. The velocity, temperature, concentration, shear stress and rate of Heat and Mass transfer are evaluated numerically for different variations of parameter.

2. FORMULATION OF THE PROBLEM

We consider a fully developed laminar convective heat and mass transfer flow of a viscous fluid through a porous medium confined in a vertical channel bounded by flat walls. We choose a Cartesian co-ordinate system O(x, y, z) with x- axis in the vertical direction and y-axis normal to the walls. The walls are taken at $y=\pm L$. The walls are maintained at constant temperature and concentration. The temperature gradient in the flow field is sufficient to cause natural convection in the flow field. A constant axial pressure gradient is also imposed so that this resultant flow is a mixed convection flow. The porous medium is assumed to be isotropic and homogeneous with constant porosity and effective thermal diffusivity. The thermo physical properties of porous matrix are also assumed to be constant and Boussinesq approximation is invoked by confining the density variation to the buoyancy term. In the absence of any extraneous force flow is unidirectional along the x-axis which is assumed to be infinite.

© 2017, IJMA. All Rights Reserved

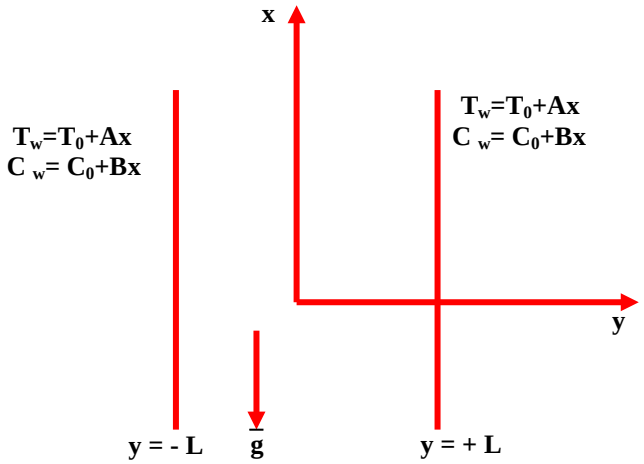

Fig.1: Configuration of the problem

The momentum, energy and diffusion equations in the scalar form are

$$-\frac{\partial p}{\partial x}+\left(\frac{\mu}{\delta}\right)\frac{\partial^2 u}{\partial y^2}-\left(\frac{\mu}{k}\right)u-\frac{\rho\delta F}{\sqrt{k}}u^2-\rho g=0 \tag{1}$$

$$\rho_0 C_p u\frac{\partial T}{\partial x}=k_f\frac{\partial^2 T}{\partial y^2}+Q_H(T_o-T) \tag{2}$$

$$u\frac{\partial C}{\partial x}=D_1\frac{\partial^2 C}{\partial y^2}-k_1 C+k_{11}\frac{\partial^2 T}{\partial y^2} \tag{3}$$

The relevant boundary conditions are

$u=0$, $T=T_w$, $C=C_w$ at $y=\pm L$ (4)

where u, T, C are the velocity, temperature and Concentration, p is the pressure ,ρ is the density of the fluid ,Cp is the specific heat at constant pressure, μ is the coefficient of viscosity, k is the permeability of the porous medium, δ is the porosity of the medium,β is the coefficient of thermal expansion, k_f is the coefficient of thermal conductivity ,F is a function that depends on the Reynolds number and the microstructure of porous medium, $\beta^\bullet$ is the volumetric coefficient of expansion with mass fraction concentration, k_1 is the chemical reaction coefficient and D_1 is the chemical molecular diffusivity, q_R is the radiative heat flux,$k_{11}$is the cross diffusivity and Q_H is the strength of the heat generating source. Here, the thermo physical properties of the solid and fluid have been assumed to be constant except for the density variation in the body force term (Boussinesq approximation) and the solid particles and the fluids are considered to be in the thermal equilibrium).

Following Tao [24] and Das *et al.* [10] we assume that the temperature and concentration of the both walls is $T_w=T_0+Ax,\ C_w=C_0+Bx$ where A and B are the vertical temperature and concentration gradients which are positive for buoyancy –aided flow and negative for buoyancy –opposed flow, respectively, T_0 and C_0 are the upstream reference wall temperature and concentration respectively. For the fully developed laminar flow in the presences of radial magnetic field, the velocity depend only on the radial coordinate and all the other physical variables except temperature, concentration and pressure are functions of y and x, x being the vertical co-ordinate. The temperature and concentration inside the fluid can be written as

$$T=T^\bullet(y)+Ax,\qquad C=C^\bullet(y)+Bx$$

We define the following non-dimensional variables as

$$u'=\frac{u}{(\nu/L)},\ (x',y')=(x,y)/L\ ,\quad p'=\frac{p\delta}{(\rho\nu^2/L^2)}\ ,\ \theta(y)=\frac{T^\bullet-T_0}{P_1AL},\quad C=,\quad \frac{C^\bullet-C_0}{P_1BL}\ ,P_1=\frac{dp}{dx} \tag{5}$$

Introducing these non-dimensional variables the governing equations in the dimensionless form reduce to (on dropping the dashes)

$$\frac{d^2u}{dy^2}=1+\delta(D^{-1})u-\delta G(\theta+NC)-\delta^2\Delta u^2 \tag{6}$$

© 2017, IJMA. All Rights Reserved

$$\frac{d^2\theta}{dy^2} - Q\theta = (P_r)u \tag{7}$$

$$\frac{d^2C}{dy^2} - \gamma C = (Sc)u \tag{8}$$

Where

$\Delta = FD^{-1/2}$ (Inertia or Forchheimer parameter) $G = \frac{\beta g A L^3}{\nu^2}$ (Grashof Number)

$D^{-1} = \frac{L^2}{k}$ (Inverse Darcy parameter) $Sc = \frac{\nu}{D_1}$ (Schmidt number) $N = \frac{\beta^{\bullet} B}{\beta A}$ (Buoyancy ratio)

$P_r = \frac{\mu C_p}{k_f}$ (Prandtl Number) $Q = \frac{Q_H L^2}{k_f}$ (Heat source parameter) $\gamma = \frac{k_1 L^2}{D_1}$ (Chemical reaction parameter)

The corresponding boundary conditions are

$$u = 0,\ \theta = 0,\ C = 0 \quad on\ y = \pm 1 \tag{9}$$

3. FINITE ELEMENT ANALYSIS

To solve these differential equations with the corresponding boundary conditions, we assume if u^i, θ^I , c^i are the approximations of u, θ and C we define the errors (residual) E_u^i, E_θ^i, E_c^i as

$$E_u^i = \frac{d}{d\eta}\left(\frac{du^i}{d\eta}\right) - D^{-1}u^i + \delta^2\Delta(u^i)^2 - \delta G(\theta^i + NC^i) \tag{10}$$

$$E_c^i = \frac{d}{dy}\left(\frac{dC^i}{dy}\right) - \gamma C^i - Scu^i \tag{11}$$

$$E_\theta^i = \frac{d}{dy}\left(\frac{d\theta^i}{dy}\right) - Q\theta^i - P_r u^i) \tag{12}$$

Where

$$u^i = \sum_{k=1}^{3} u_k\psi_k \qquad C^i = \sum_{k=1}^{3} C_k\psi_k \qquad \theta^i = \sum_{k=1}^{3} \theta_k\psi_k \tag{13}$$

These errors are orthogonal to the weight function over the domain of e^i under Galerkin finite element technique we choose the approximation functions as the weight function. Multiply both sides of the equations (10-12) by the weight function i.e. each of the approximation function ψ_j^i and integrate over the typical three nodded linear element (η_e, η_{e+1}) we obtain

Where

$$\int_{\eta_e}^{\eta_{e+1}} \left(\frac{d}{d\eta}\left(\frac{du^i}{d\eta}\right) - D^{-1}u^i + \delta^2\Delta(u^i)^2 - \delta G(\theta^i + NC^i\right)\psi_j^i dy = 0 \tag{14}$$

$$\int_{\eta_e}^{\eta_{e+1}} \left(\frac{d}{dy}\left(\frac{dC^i}{dy}\right) - \gamma C^i - Scu^i\right)\psi_j^i dy = 0 \tag{15}$$

$$\int_{\eta_e}^{\eta_{e+1}} \left(\frac{d}{dy}\left(\frac{d\theta^i}{dy}\right) - Q\theta^i - P_r u^i\right)\psi_j^i dy = 0 \tag{16}$$

Choosing different Ψ_j^i's corresponding to each element η_e in the equation (14) - (16) yields a local stiffness matrix of order 3×3 in the form

$$(f_{i,j}^k)(u_i^k) - \delta G(g_{i.j}^k)(\theta_i^k + NC_i^k) + \delta D^{-1}(m_{i.j}^k)(u_i^k) + \delta^2 \mathrm{A}(n_{i.j}^k)(u_i^k) = (Q_{i,j}^k) + (Q_{2,j}^k) \tag{17}$$

© 2017, IJMA. All Rights Reserved

$$((e_{i,J}^k)-\gamma)(C_i^k)-Sc(m_{i.j}^k)(u_i^k)=R_{1J}^k+R_{2J}^k \quad (18)$$

$$((l_{iJ}^k)-Q)(\theta_i^k)-P_r(t_{iJ}^k)(u_i^k)=S_{1,J}^k+S_{2,J}^k \quad (19)$$

Where

$\left(f_{i,J}^k\right)$, $\left(g_{i,J}^k\right),\left(m_{i,J}^k\right),\left(n_{i,J}^k\right),\left(e_{i,J}^k\right),\left(t_{iJ}^k\right)$ are3×3matricesand$\left(Q_{2,J}^k\right),\left(Q_{1,J}^k\right),\left(R_{2,J}^k\right),\left(R_{1J}^k\right),\left(S_{2J}^k\right)$ and $\left(S_{1J}^k\right)$ are 3×1 column matrices and such stiffness matrices ((17)–(19)) in terms of local nodes in each element are assembled using inter element continuity and equilibrium conditions to obtain the coupled global matrices in terms of the global nodal values of u, θ & C. The resulting coupled stiffness matrices are solved by iteration process. This procedure is repeated till the consecutive values of u_i's, θ_i's and C_i's differ by a preassigned percentage.

4. SHEAR STRESS, NUSSELT NUMBER AND SHERWOOD NUMBER

The shear stress on the boundaries $y=\pm 1$ is given by $\tau_{y=\pm L}=\mu\left(\frac{du}{dy}\right)_{y=\pm L}$

In the non-dimensional form is $\tau_{y=\pm 1}=\left(\frac{du}{dy}\right)_{y=\pm 1}$

The rate of heat transfer (Nusselt Number) is given by $Nu_{y=\pm i}=\left(\frac{d\theta}{dy}\right)_{y=\pm 1}$

The rate of mass transfer (Sherwood Number) is given by $Sh_{y=\pm 1}=\left(\frac{dC}{dy}\right)_{y=\pm 1}$

COMPARISON:

In the absence of Heat Sources (Q=0) the results are good agreement with Rao (2016).

Table-1

Parameters		Rao Results (24a)			Present Results (Q=0)		
N	γ	τ(+1)	Nu(+1)	Sh(+1)	τ(+1)	Nu(+1)	Sh(+1)
1	0.5	0.905897	0.0182438	0.0495379	0.905898	0.0182439	0.0495378
2	0.5	0.898419	0.0181713	0.0449901	0.898418	0.0181714	0.0449902
-0.5	0.5	0.911432	0.0181152	0.0480718	0.911434	0.0181154	0.0480719
-1.5	0.5	0.919737	0.0181098	0.0491045	0.919738	0.0181097	0.0491047
1	1.5	0.91984	0.0181720	0.0547955	0.91985	0.0181722	0.0547956
1	-0.5	0.919767	-.0181751	0.0649491	0.919768	-.0181752	0.0649492
1	-1.5	0.91972	-0.018177	0.0715908	0.91971	-0.018178	0.0715909

5. DISCUSSION OF THE NUMERICAL RESULTS

In order to gets physical Insight into the problem we have carried out numerical calculations for non-dimensional velocity, temperature and spices concentration, skin-friction, Nusselt number and Sherwood number by assigning some specific values to the parameters G, D^{-1}, N, Sc, Q, γ, Δ entering into the problem.

Effects of parameters on velocity profiles:

The variation of axial velocity with different parameters shows that u<0 i.e. it is in the downward direction of the channel. Fig.2a shows the variation of the velocity with Grashof number G at any point in the flow region. It is observed from the profiles that the velocity decreases with increase in the buoyancy parameter (G). The maximum of u occurs at y=0.0. Fig.3a represents the u with the inverse Darcy parameter (D^{-1}). The axial velocity reduces with increase in D^{-1}. This is due to the fact that the presence of the porous medium enhances the resistance to the flow resulting in the reduction of the velocity field. Fig.4a exhibits the variation of u with buoyancy ratio (N). It is found that when the molecular buoyancy force dominates over the thermal buoyancy force the axial velocity decreases when the buoyancy forces are in the same direction and for the forces are in opposite directions, it increases in the flow region.

© 2017, IJMA. All Rights Reserved

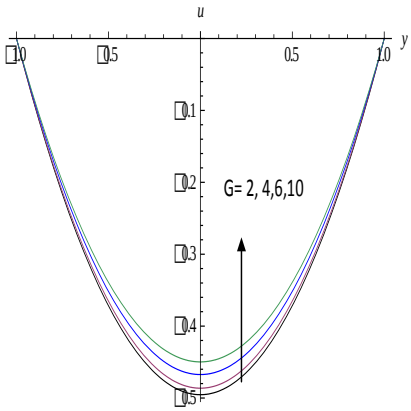

Fig. 2a: Variation of u with G
D^{-1}=0.2, Sc=1.3, N=1, Q=0.5, γ=0.5, Δ=2

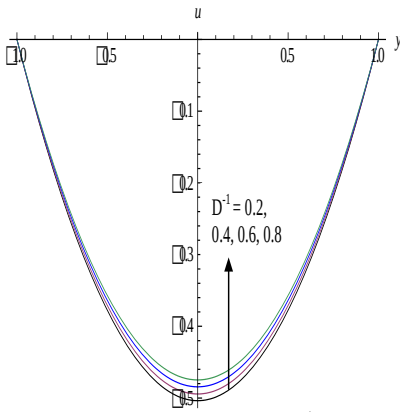

Fig. 3a: Variation of u with D^{-1}
G=2, Sc=1.3, N=1, Q=0.5, γ=0.5, Δ=2

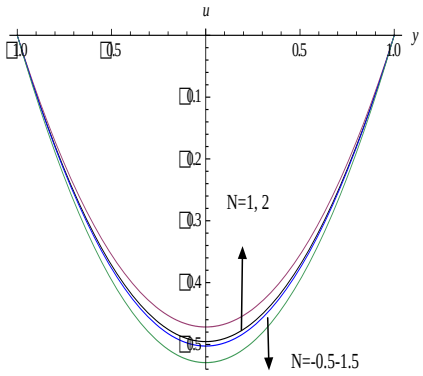

Fig. 4a: Variation of u with N
G=2, D^{-1}=0.2, Sc=1.3, N=1, Q=0.5, γ=0.5, Δ=2

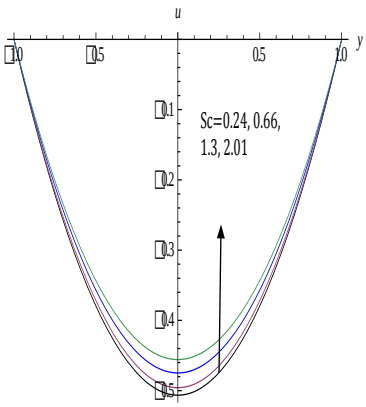

Fig. 5a: Variation of u with Sc
G=2, D^{-1}=0.2, N=1, Q=0.5, γ=0.5, Δ=2

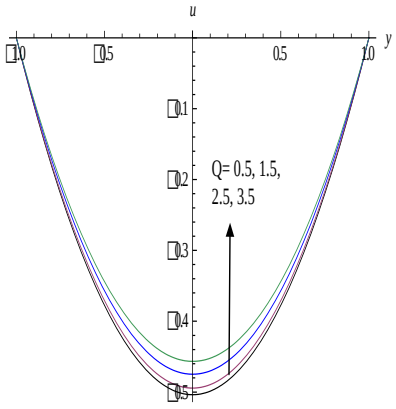

Fig. 6a: Variation of u with Q>0
G=2, D^{-1}=0.2, Sc=1.3, N=1, γ=0.5, Δ=2

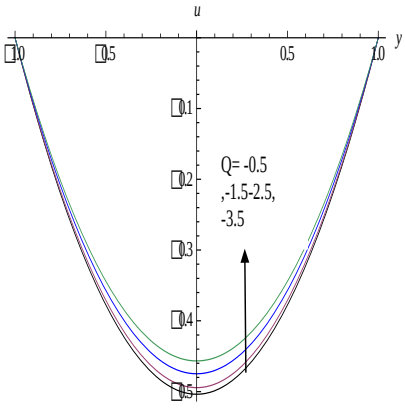

Fig. 7a : Variation of u with Q<0
G=2, D^{-1}=0.2, Sc=1.3, N=1, γ=0.5, Δ=2

Fig.5a shows the variation of u with Schmidt number (Sc).It is found that the velocity reduces with increases in Sc. This is due to the fact that increasing Sc means reducing molecular diffusivity, therefore lesser the molecular diffusivity smaller the velocity in the fluid region. Fig.6a and 7a shows the variation of u with heat source parameter (Q). It is found that an increase on the strength of the heat generating/absorption source smaller the velocity in the entire flow region.

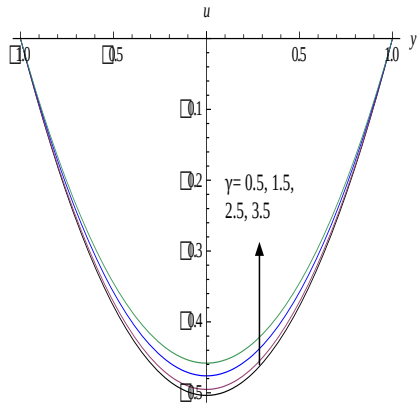

Fig. 8a : Variation of u with γ>0
G=2, D^{-1}=0.2,Sc=1.3,N=1, Q=0.5, Δ=2

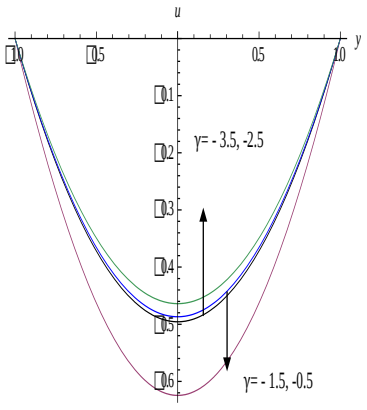

Fig. 9a : Variation of u with γ<0
G=2, D^{-1}=0.2,Sc=1.3,N=1, Q=0.5, Δ=2

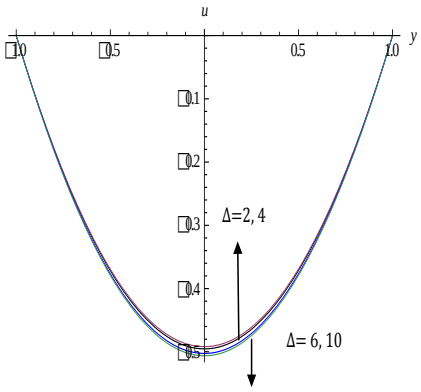

Fig. 10a: Variation of u with Δ
G=2, D^{-1}=0.2, Sc=1.3, N=1, Q=0.5, γ=0.5

The effect of chemical reaction parameter (γ) on u is exhibited in Fig.8a and 9a. It is found that the axial velocity enhances with increase in γ in the entire flow region in the degenerating chemical reaction case while in the generating chemical reaction case the velocity reduces in the flow region. Fig.10a represents the variation of u with Forchheimer number (Δ). An increase in Δ increases the velocity in the flow region. This is due to the fact that increasing Δ increases the thickness of the momentum boundary layer which in turn increases the velocity in the flow region.

© 2017, IJMA. All Rights Reserved

Effects of parameters on temperature profiles:

The non-dimensional temperature (θ) is shown in figs.2b-10b for different parametric representation. We follow the convention that the non-dimensional temperature (θ) is positive/negative according as the actual temperature $(T^{\bullet})$ is greater/lesser than the reference temperature T_0.

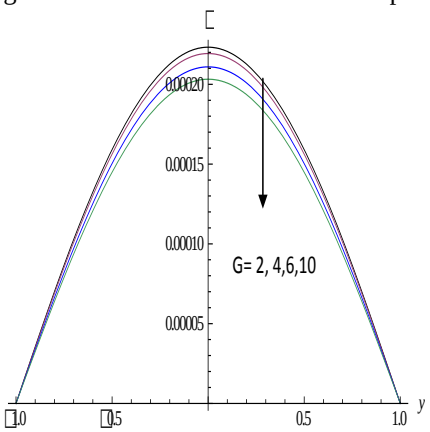

Fig. 2b: Variation of θ with G
D^{-1}=0.2, Sc=1.3, N=1,Q=0.5, γ=0.5, Δ=2

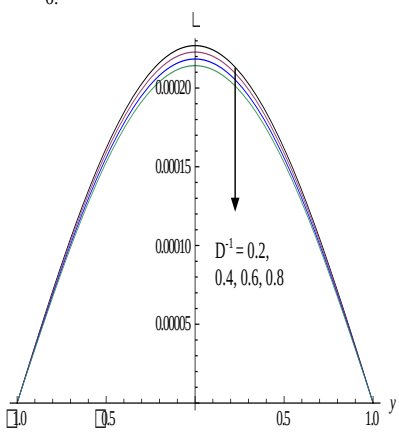

Fig. 3b: Variation of θ with D^{-1}
G=2, Sc=1.3, N=1, Q=0.5, γ=0.5, Δ=2

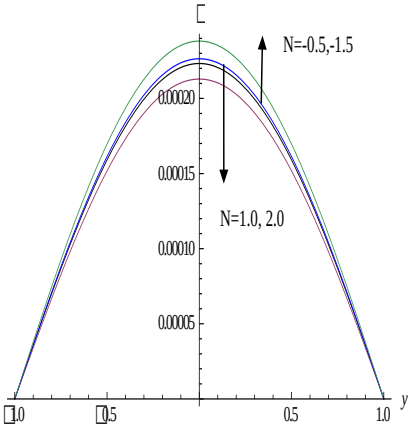

Fig. 4b: Variation of θ with N
G=2, D^{-1}=0.2, Sc=1.3, N=1,Q=0.5, γ=0.5, Δ=2

Fig.2b exhibits the temperature with G. It is found that the actual temperature reduces with increase in Grashof number with maximum attained at y=0. With reference to D^{-1} we find that the actual temperature decreases with increasing values of D^{-1}. This is due to the fact that the thickness of the boundary layer decreases owing to the Darcy drag developed by the porous medium (Fig.3b). Fig.4b shows the variation of θ with buoyancy ratio (N). It is observed from the profiles that when the molecular buoyancy force dominates over the thermal buoyancy force the actual temperature reduces when the buoyancy forces are in the same direction and for the forces are in opposite directions it increases in the floe region. Fig.5b represents θ with Sc .It is found that lesser the molecular diffusivity lesser the actual temperature in the entire flow region. Fig.6band 7b exhibits the variation of θ with heat source parameter (Q). It is observed from the profiles that an increase in the strength of the heat generating/absorbing source leads to reduce in the actual temperature in the flow region.

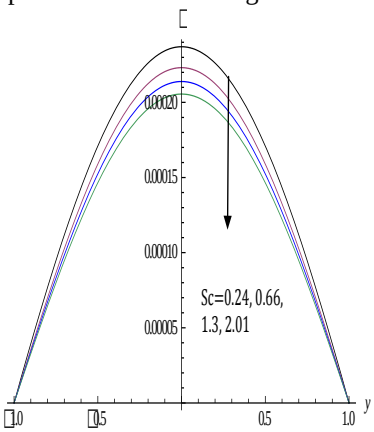

Fig. 5b: Variation of θ with Sc
G=2, D^{-1}=0.2, N=1, Q=0.5, γ=0.5, Δ=2

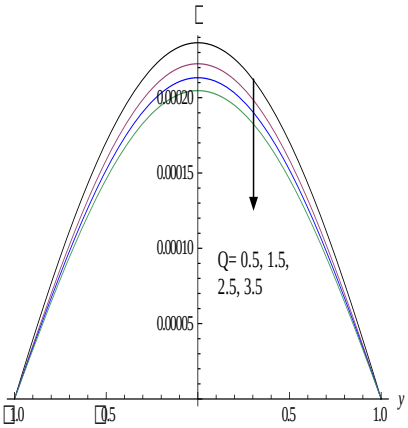

Fig. 6b: Variation of θ with Q>0
G=2, D^{-1}=0.2, Sc=1.3, N=1, γ=0.5, Δ=2

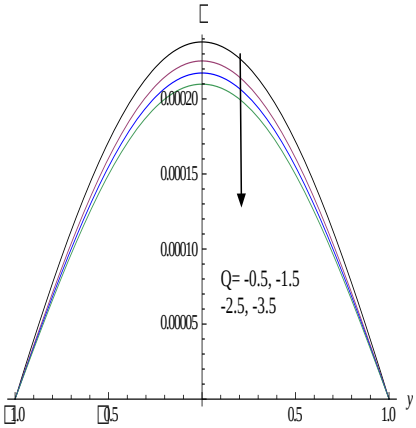

Fig. 7b : Variation of θ with Q<0
G=2, D^{-1}=0.2, Sc=1.3, N=1, γ=0.5, Δ=2

Fig.8b and 9b represents θ with chemical reaction parameter (γ). From the profiles we find that the actual temperature reduces with increase in γ in the degenerating chemical reaction case (γ>0). In the generating chemical reaction case (γ<0) the actual temperature increases with in |γ|≦1.5 and higher |γ|2≥.5 it reduces in the flow regi on. Fig.10b shows the variation of θ with Forchheimer number (Δ). As the Forchheimer increases there is a significant enhancement in the thermal boundary layer with a fall in the actual temperature throughout the flow region. Thus the inclusion of the inertia effects is to enhance the actual temperature in the flow region.

© 2017, IJMA. All Rights Reserved

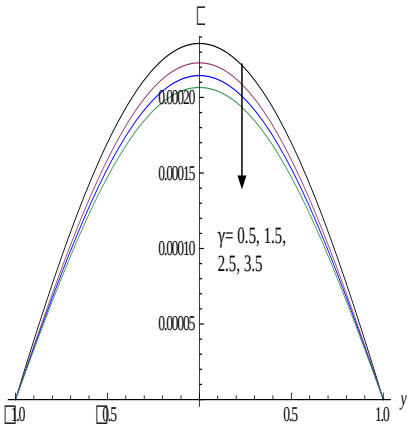

Fig. 8b: Variation of θ with γ>0
G=2, D^{-1}=0.2, Sc=1.3,N=1, Q=0.5, Δ=2

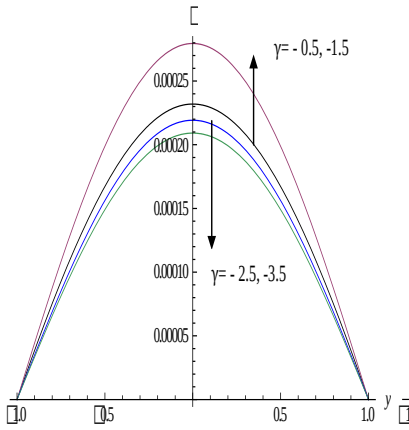

Fig. 9b : Variation of θ with γ<0
G=2, D^{-1}=0.2,Sc=1.3,N=1, Q=0.5, Δ=2

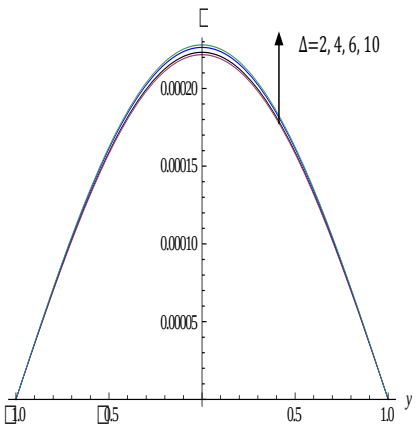

Fig. 10b: Variation of θ with Δ
G=2, D^{-1}=0.2, Sc=1.3, N=1, Q=0.5, γ=0.5

Effects of parameters on concentration profiles:

The non-dimensional concentration (C) is shown in figs.2c-10c for different parametric variations. We follow the convention that the non-dimensional concentration (C) is positive/negative according as the actual concentration ($C^{\bullet}$) is greater/lesser than the reference concentration (C_o) .

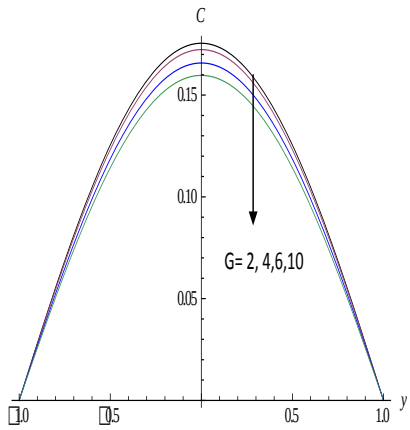

Fig. 2c: Variation of C with G
D^{-1}=0.2, Sc=1.3, N=1, Q=0.5, γ=0.5, Δ=2

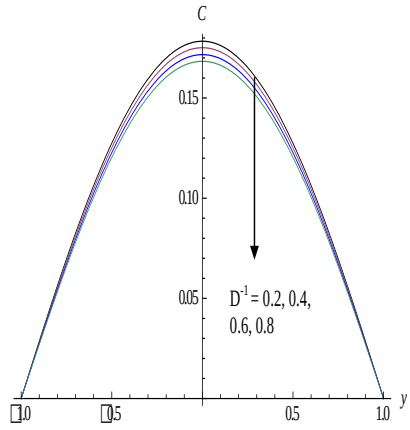

Fig. 3c: Variation of C with G
D^{-1}=0.2, Sc=1.3, N=1, Q=0.5, γ=0.5, Δ=2

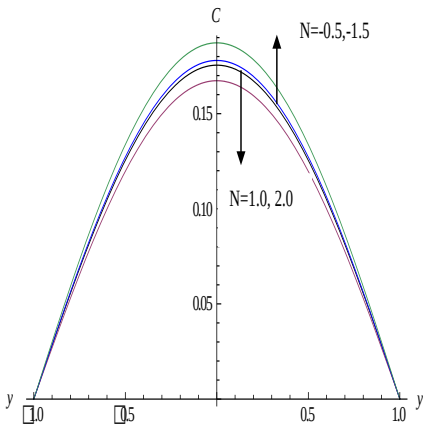

Fig. 4c: Variation of C with N
G=2, D^{-1}=0.2, Sc=1.3, N=1, Q=0.5, γ=0.5, Δ=2

Fig.2c shows the variation of Concentration with Grashof number G. It can be seen from the profiles that the actual concentration reduces with increasing G. Fig.3c represents C with D^{-1}. We find that lesser the permeability of the porous medium smaller the actual concentration in the entire flow region. Fig.4c shows the variation of C with buoyancy ratio N. We find that when the molecular buoyancy force dominates over the thermal buoyancy force the actual concentration decreases when the buoyancy forces are in the same direction and for the forces acting in the opposite directions, it enhances in the flow region.

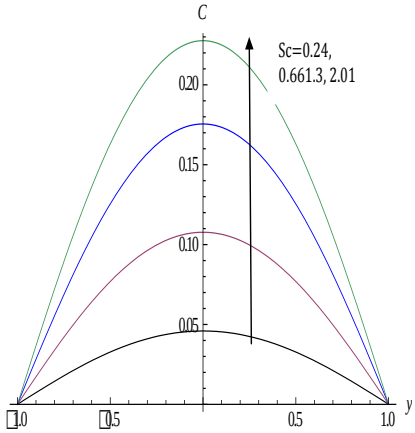

Fig. 5c : Variation of C with Sc
G=2, D^{-1}=0.2, N=1,Q=0.5, γ=0.5, Δ=2

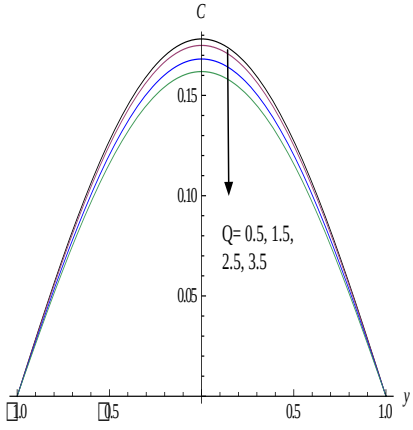

Fig. 6c: Variation of C with Q>0
G=2, D^{-1}=0.2, Sc=1.3, N=1, γ=0.5, Δ=2

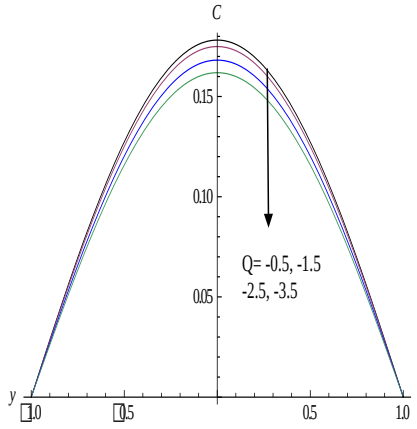

Fig. 7c: Variation of C with Q<0
G=2, D^{-1}=0.2, Sc=1.3, N=1, γ=0.5, Δ=2

© 2017, IJMA. All Rights Reserved

Fig.5c shows the variation of C with Sc. It can be seen from the profiles that the actual concentration enhances with increase in Sc. Fig.6c and 7c shows the variation of C with heat source parameter (Q). An increase in the strength of the heat generating/absorbing source leads to a depreciation in the actual concentration.

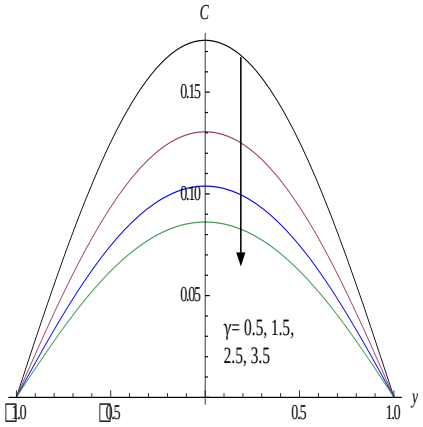

Fig. 8c: Variation of C with γ>0
G=2, D^{-1}=0.2, Sc=1.3, N=1, Q=0.5, Δ=2

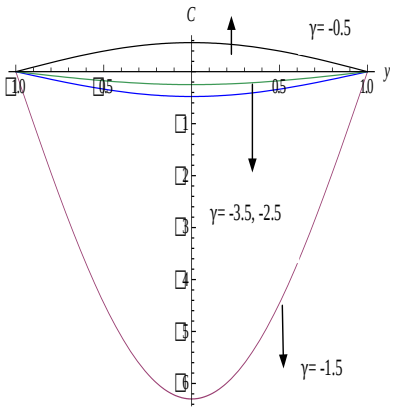

Fig. 9c: Variation of C with γ<0
G=2, D^{-1}=0.2, Sc=1.3, N=1, Q=0.5, Δ=2

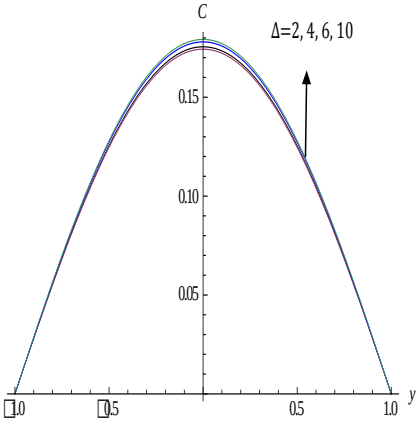

Fig. 10c: Variation of C with Δ
G=2, D^{-1}=0.2, Sc=1.3, N=1, Q=0.5, γ=0.5

Fig.8c and 9c shows the variation of C with Chemical reaction parameter (γ). It can be seen from the profiles that the actual concentration reduces in the degenerating chemical reaction case (γ>0) in the entire flow region. Also we find that the actual concentration reduces with increase in $|\gamma| \leq 1.5$ and higher $|\gamma| \geq 2.5$, we notice an enhancement in the actual concentration. Fig.10c exhibits the variation of C with Forchheimer number (Δ). As the Forchheimer number increases there is a marginal increase in the actual concentration. This is due to the fact the enhancement of Forchheimer number increases the thickness of the thermal boundary layer.

Effects of parameters on Skin friction, Nusselt number and Sherwood number:

The Skin friction, the rate of heat and mass transfer at the boundaries y=±1 is exhibited in table-2.

Table -2

		τ(1)	τ (-1)	Nu(1)	Nu(-1)	Sh(1)	Sh(-1)
G	**2**	0.926897	-0.926897	0.0181438	-0.0181438	0.0525079	-0.0525079
	4	0.879052	-0.879052	0.0169699	-0.0169699	0.0459606	-0.0459606
	6	0.867768	-0.867768	0.0159654	-0.0159654	0.0428572	-0.0428572
	10	0.845212	-0.845212	0.0139551	-0.0139551	0.0396514	-0.0396514
D^{-1}	**0.2**	0.926897	-0.926897	0.0181438	-0.0151438	0.0525079	-0.0525079
	0.4	0.912073	-0.912073	0.0188694	-0.0159694	0.0540453	-0.0540453
	0.6	0.914682	-0.914682	0.0192117	-0.0162117	0.0561453	-0.0561453
	0.8	0.917703	-0.917703	0.0196318	-0.0165018	0.0593351	-0.0923351
N	**1.0**	0.926897	-0.926897	0.0182438	-0.0182438	0.0525079	-0.0525079
	2.0	0.898419	-0898419	0.0181713	-0.0181713	0.0449901	-0.0449901
	-0.5	0.901432	-0.901432	0.0181052	-0.0181052	0.0490718	-0.0490771
	-1.5	0.929737	-0.929737	0.0180998	-0.0180998	0.0511045	-0.0501045
Sc	**0.24**	0.944437	-0.946837	0.0181038	-0.0181038	0.0105079	-0.0105079
	0.66	0.938782	-0.938782	0.0181282	-0.0181282	0.0364383	-0.0364383
	1.3	0.926897	-0.926897	0.0181438	-0.0181438	0.0525079	-0.0525079
	2.01	0.915889	-0.915889	0.0182293	-0.0182293	0.078226	-0.078226
Q	**0.5**	0.926897	-0.926897	0.0181438	-0.0105916	0.0525079	-0.0525079
	1.5	0.899824	-0.899824	0.0181729	-0.0181729	0.0500227	-0.0500227
	-0.5	0.919932	-0.919932	-0.004783	0.00478372	0.0627414	-0.0627414
	-1.5	0.919967	-0.919967	-0.012435	0.0124359	0.0643143	-0.0433143
γ	**0.5**	0.926897	-0.926897	0.0181438	-0.0181438	0.0525079	-0.0525079
	1.5	0.91984	-0.91984	0.0181122	-0.0181122	0.0517955	-0.0517955
	-0.5	0.919767	-0.919767	0.0181751	-0.0181751	0.0649491	-0.0649491
	-1.5	0.91972	-0.91972	0.018177	-0.018177	0.0715908	-0.0715908
Δ	**2**	0.926897	-0.926897	0.0181438	-0.0181438	0.0525079	-0.0525079
	4	0.919835	-0.919835	0.0196092	-0.0196092	0.0474431	-0.0474431
	6	0.919834	-0.91983	0.0200284	-0.0200284	0.0452547	-0.0452547
	10	0.919822	-0.919822	0.0285406	-0.0285406	0.0439482	-0.0439482

© 2017, IJMA. All Rights Reserved

From the tabular values we find that an increase in G or Sc reduces the skin friction on both the wall $y=\pm 1$. Lesser the permeability of the porous medium the skin friction increases on the both the walls. The skin friction reduces on $y=\pm 1$ with increase in the strength of the heat generating while it reduces with strength of the heat absorption source .When the molecular buoyancy force dominates over the thermal buoyancy force the skin friction reduces on the walls when the buoyancy forces are in the same direction and for the forces acting in opposite directions it increases on the walls. With reference to the chemical reaction parameter (γ) we find that the skin friction enhances on both the walls in the degenerating chemical reaction case and in the generating chemical reaction case it reduces on the walls. As the Forchheimer number increases ($\Delta \leq 0.1$) the skin friction enhances on $y=\pm 1$ and reduces for higher $\Delta \geq 0.3$ on both the walls. The rate of heat transfer (Nusselt number) reduces with increase in G and enhances with D^{-1}or Δ. It reduces on the walls with increasing in the buoyancy ratio (N) irrespective of the directions of the buoyancy forces. The variation of Nu with Sc shows that lesser the molecular diffusivity ($Sc \leq 0.66$) smaller Nu on $y=\pm 1$ while for further lowering of the molecular diffusivity ($Sc \geq 1.3$) larger the skin friction on the walls. The magnitude of Nu reduces on $y=\pm 1$, with increase in the strength of the heat generating/ absorption source .With respect to the chemical reaction parameter (γ) we find that the magnitude of Nu reduces in the degenerating chemical reaction case and enhances in the generating chemical reaction case on both the walls. The rate of mass transfer (Sherwood number) reduces with increase G or Δ and enhances with D^{-1} or Sc on both the walls. An increase in $Q>0$ reduces Sh on $y=\pm 1$ while a reversed effect is noticed for $Q<0$.With respect to the chemical reaction parameter (γ) we find that the rate of mass transfer reduces on $y=\pm 1$ in degenerating chemical reaction case while in the generating case it increases on the walls. The rate of mass transfer reduces with increase in $N>0$ and enhances with $N<0$ on both the walls.

6. CONCLUSIONS

The non-linear coupled equations governing the flow, heat and mass transfer have been solved by employing Galerkin finite element technique. The velocity, temperature, concentration, skin friction and the rate of heat and mass transfer on the walls have been discussed for different variations of the parameters. The important conclusions of the analysis are:

1) An increase in the buoyancy parameter (G) reduces the velocity, temperature and concentration. The skin friction, the rate of heat and mass transfer on reduces on the walls.
2) Lesser the permeability of the porous medium smaller the velocity, concentration, temperature and larger the skin friction rate of heat and mass transfer on the walls.
3) The velocity, temperature and concentration reduces with increase in the buoyancy ratio (N)>0 while for N<0, the velocity and temperature increases, the concentration reduces in the flow region. The skin friction, Nusselt number and Sherwood number reduces on the walls with N>0 and for N<0, the skin friction and Sherwood number enhances while the Nusselt number reduces on the walls.
4) Lesser the molecular diffusivity smaller the velocity and concentration and smaller the temperature. The skin friction and Nusselt Number reduces and the Sherwood number increases with Sc.
5) An increase in the strength of the heat generating / absorbing (Q) reduces the velocity, temperature and concentration. The skin friction and Sherwood number reduces on the walls with Q>o while for Q<0, they enhance on $y=\pm 1$.
6) The temperature and concentration reduce while the velocity reduces with $\gamma>0$ while for $\gamma<0$, they increase with $|\gamma| \leq 1.5$ and decreases with $|\gamma| \geq 2.5$ in the entire flow region. The rate of heat and mass transfer reduce and the skin friction increases on the walls with increase in $\gamma>0$ while a reversed effect is noticed with $\gamma<0$.
7) An increase in Forchheimer parameter (Δ) increases the velocity, temperature and concentration.

7. REFERENCES

[1] Alam M.S., Rahman M.M., Sattar M.A: MHD free convection heat and Mass transfer flow past an inclined surface with heat generation, Thamasat, Int. J. Sci. Tech 11(4) pp.1-8 (2006).
[2] Al-Nimir, M.A, Haddad, O.H: Fully developed free convection in open-ended vertical chasnnels partially filled with porous material,J.Porous Media,V.2,pp.179-189(1999).
[3] Barletta,A: Analysis of combined forced and free flow in a vertrical channel with viscous dissipation and isothermal-isoflux boundary conditions, ASME.J.Heat Transfer, V,121,pp.349-356(1999).
[4] Barletta,A,Magyari,E and Kellaer,B:Dual mixed convection flows in a vertical channel.,INny.J.Heat and Mass Transfer,V.48,pp.4835-4845(2005).
[5] Barletta,A,Celli,M and Magtyari,E and Zanchini,E: Buoyany MHD flows in a vertical channel:the levitation regime.,Heat and Mass Transfer,V.44,pp.1005-1013(2007).
[6] Beckermann,C.Visakanta,r and.Ramadhyani,S: A numerical study of non-Darcian natural convection in a vertical enclosure filled with a porous medium., Numerical Heat transfer 10, pp.557-570, (1986).
[7] Cebeci,T,Khattab,A.A and LaMont,R: Combined natural and forced convection in a vertical ducts, in:Proc.7th Int. Heat Transfer Conf.,V.3,pp.419-424(1982).
[8] Chamka, A.J: Unsteady MHD Convective Heat and Mass transfer past a semi-infinite vertical permeable moving plate with heat absorption Int. J. Eng. Sci. 24, pp.217-230 (2004).

© 2017, IJMA. All Rights Reserved

[9] Cheng: Heat transfer in geothermal systems. Adv.Heat transfer 14,1-105(1978).
[10] Das,S., Jana,R.N and Makinde,O.D : Mixed convective magnetohydrodynamic flow in a vertical channel filled with Nanofluid., Eng.Sci.and Technology-an International journal;,V,18,pp.244-255(2015).
[11] Datta,N anfd Jana,R.N: Effect of wall conductance on hydromagnetic convection of a radiation gas in a vertical channel., Int.J.Heat Mass Transfer,V.19,pp.1015-1019(1974).
[12] Deepti,J, Prasada Rao,D.R.V: Finite element analysis of chemically reaction effect on Non-Darcy convective heat and mass transfer flow through a porous medium in a vertical channel with constant heat sources.,Int.J.Math.Arch,V.3(11),pp.3885-3897(2012).
[13] Gill,W.N and Del Casal,A: A theoretical investigation of natural convection effects in a forced horizontal flows,AIChE J,V.8,pp.513-518(1962).
[14] Greif, R, Habib, I.S and Lin,J.c: Laminar convection of a radiating gas in a vertical channel, J.Fluid. Mech., V.46, p.513 (1971).
[15] Gupta,P.S and Gupta, A.S:Radiation effect on hydromagnetic convection in a vertical channel., Int.J.heat Mass Transfer,V.127,pp.1437-1442(1973).
[16] Hady F.M., Mohamed R.A., Mahdy A: MHD free convective flow along a vertical wavy surface with heat generation or absorption effect Int. Comm. Heat Mass transfer, 33 (2006).
[17] Hossain M.A., Molla M.M., Yaa L.S: Natural convective flow along a vertical wavy surface temperature in the presence of heat generation/ absorption, Int. J. Thermal Science 43, pp157-163 (2004).
[18] Kalidas.N. and Prasad, V: Benard convection in porous media Effects of Darcy and Pransdtl Numbers, Int. Syms. Convection in porous media, non-Darcy effects, proc.25th Nat. Heat Transfer Conf.V.1,pp. 593-604 (1988).
[19] Kamalakar,P.V.S Prasada Rao,D.R.V and Raghavendra Rao,R: Finite element analysis of chemical reaction effect on Non-Darcy convective heat and mass transfer flow through a porous medium in a vertical channel with heat sources., Int.J.Appl.Math and Mech,V,8(13), pp.13-28(2012).
[20] Laurait,G and.Prasad,V: Natural convection in a vertical porous cavity a numerical study of Brinkman extended Darcy formulation., J.Heat Transfer.pp.295-320(1987).
[21] Ostrach,S:Combined natural and forced convection laminar flow and heat transfer of fluid with and without heat sources in channels with linearly varying wall temperature, NACA TN,3141,(1954).
[22] Prasad, V.and Tuntomo, A: Inertia Effects on Natural Convection in a vertical porous cavity, numerical Heat Transfer, V.11, pp.295-320 (1987).
[23] Prasad.V, F.A,Kulacki and M.Keyhani: Natural convection in a porous medium" J.Fluid Mech.150p.89-119 (1985).
[24] Poulikakos D., and Bejan, A: The Departure from Darcy flow in Nat. Convection in a vertical porous layer, physics fluids V.28, pp.3477-3484 (1985).
[24a]Sreenivasa Rao, P: Non-Darcy convective heat and mass transfer flow in a vertical channel, Paper accepted for publication in IISTE, Nov (2016).
[25] Tao,L.N:On combined and forced convection in channels, ASME J.Heat Transfer, V.82, pp.233-238(1960).
[26] Tien, D., and Hong, J.T: Natural convection in porous media under non-Darcian and non-uniform permeability conditions, hemisphere, Washington.C. (1985).
[27] Tong, T.L and Subramanian, E: A boundary layer analysis for natural correction in porous enclosures: use of the Brinkman-extended Darcy model, Int.J.Heat Mass Transfer.28, pp. 563-571 (1985).
[28] Umadevi,B,Sreenivas,G,Bhuvana vijaya,R and prasada Rao,D.R.V: Finite element analysis of chemical reaction effect on Non-Darcy mixed convective double diffusive heat transfer flow through a porous medium in a vertical channel with constant heat sources., Adv. Appl. Sci. Res. V.3 (5), pp.2924-2939(2012).
[29] Vafai, K., Tien, C.L: Boundary and Inertia effects on flow and Heat Transfer in Porous Media, Int. J. Heat Mass Transfer, V.24. Pp.195-203 (1981).
[30] Vafai, K., Thyagaraju, R: Analysis of flow and heat Transfer at the interface region of a porous medium, Int. J. Heat Mass Trans., V.30pp.1391-1405 (1987).
[31] Vajravelu K, Hadjnicolaou, A: Heat transfer in a viscous fluid over a stretching sheet with viscous dissipation and internal heat generation, Int. Comm. Heat Mass transfer 20, pp.417-430 (1993).
[32] Wirtz,R.A and McKinley,P: Buoyancy effects on downward laminar convection between parallel plates Fundamental of forced and mixed convection, ASME HTD,V.42,pp.105-112(1985).

Source of support: Nil, Conflict of interest: None Declared.

[Copy right © 2016. This is an Open Access article distributed under the terms of the International Journal of Mathematical Archive (IJMA), which permits unrestricted use, distribution, and reproduction in any medium, provided the original work is properly cited.]